

BBA 42882

Separation and characterization of stroma and grana membranes – evidence for heterogeneity in antenna size of both Photosystem I and Photosystem II

Eva Andreasson ^a, Per Svensson ^a, Claes Weibull ^b and Per-Åke Albertsson ^a

^a Department of Biochemistry and ^b Department of Microbiology, University of Lund, Lund (Sweden)

(Received 27 April 1988)

(Revised manuscript received 5 July 1988)

Key words: Thylakoid membrane organization; Antenna size; Photosystem heterogeneity; Phase partition; (Spinach chloroplast)

A rapid procedure to fractionate the thylakoid membrane into two well-separated vesicle populations, one originating from the grana and the other from the stroma-membrane region, has been developed. This was achieved by sonication of thylakoids present in an aqueous two-phase system followed by partitioning either by countercurrent distribution or by a batch procedure in three steps. The membrane populations were analysed according to their composition and photochemical activities. The grana membranes comprise, on chlorophyll basis, about 60% of the thylakoid material and are enriched in PS II, but also contain some PS I, while the stroma membranes comprise about 40% and are enriched in PS I, but also contain some PS II. Cytochrome *f* was slightly enriched in the grana-derived vesicle fraction. The properties of both PS I and PS II differ between the two populations. The PS I of the grana fraction (PS I_α) reached half-saturation at about half the light intensity of the PS I in the stroma-membrane fraction (PS I_β). The rate of P-700 photooxidation under low light illumination was higher for PS I_α than for PS I_β (30% larger rate constant), showing that PS I_α has a larger antenna. The PS II of the grana fraction (PS II_α) reached half-saturation at half the light intensity compared to the PS II of the stroma-membrane fraction (PS II_β). The results show that the grana-derived membranes contain PS I_α and PS II_α which have larger functional antenna sizes than the corresponding PS I_β and PS II_β of the stroma membranes. The results suggest that the photosystems of the grana are designed to allow effective electron transport both at low and high light intensities, while the stroma-membrane photosystems mainly work at high light intensities as a supplement to the grana systems.

Abbreviations: CCD, countercurrent distribution; Chl, chlorophyll; DCMU, 3-(3,4-dichlorophenyl)-1,1-dimethylurea; DCIP, 2,6-dichlorophenolindophenol; PpBQ, phenyl-*p*-benzoquinone; P-700, reaction center of PS I; PS I, PS II, Photosystem I, II; SDS, sodium dodecylsulphate; Tricine, *N*-[2-hydroxy-1,1-bis(hydroxymethyl)ethyl]glycine.

Correspondence: P.A. Albertsson, Department of Biochemistry, University of Lund, P.O. Box 124, S-221 00 Lund, Sweden.

Introduction

Fragmentation of the photosynthetic membrane followed by separation and biochemical characterization of the fragments constitutes a successful approach to the study of the structure and function of the photosynthetic apparatus. The pioneering work by Michel and Michel-Wolwertz [1] and Sane et al. [2] using mechanical press

treatment, Jacobi and Lehmann [3] using sonication and Anderson and Boardman [4], using detergents, demonstrated that the photochemical systems, PS I and PS II, could be partially separated. The PS I was highly enriched in a light centrifugal fraction while both PS II and PS I were found in a heavier fraction. Electron microscope studies [2] suggested that the PS-I-rich vesicles originated from the stroma membranes, while the heavier PS-II- and PS-I-containing fraction derived from the grana region, and is also often named the grana fraction. These results have since been confirmed by many workers. Furthermore, the grana fraction can be separated into highly enriched PS II vesicles and PS-I-enriched vesicles by press treatment and partitioning in aqueous two-phase systems [5]. The PS-II-enriched vesicles have an inside-out conformation [6–8] and are supposed to be formed, under stacking conditions, by fusion between neighbouring appressed membranes of the partition region [9]. From these studies, and also from immunoelectron microscopical investigations [10–12], there has emerged a picture of an almost complete lateral segregation of PS I and PS II in the thylakoid membrane, with PS I localized in the stroma-exposed domains and PS II in the partition region [13,14].

It should be pointed out, however, that the separation of the two photosystems after mechanical press treatment is not complete [5,15–17] and that the structure of the thylakoid membrane is probably more complicated. It is true that small PS I vesicles almost lacking PS II [1–3] and PS II vesicles almost lacking PS I [18–23] can be isolated, but in both cases the yield of these particles is often only a few per cent. Furthermore, there are two classes of PS II, PS II_α and PS II_β, which differ in their antenna size and membrane localization [24–26]. PS II_α has the larger antenna, is found in the inside-out vesicles and is hence localized in the appressed partition regions, while PS II_β, with its smaller antenna size, is found in the light fraction, and hence localized in the stroma membrane [25]. According to these studies, about 25% of the PS II reaction centers are localized in the stroma region.

Our aim in this study was to characterize the two photosystems present in both the grana and stroma membranes. To this end we developed a

rapid procedure for the quantitative separation of the thylakoid membrane into two membrane fractions which we conclude are derived from the grana and stroma membranes, respectively. The grana-membrane fraction comprises about 60% of the thylakoid material and contains PS II_α and some PS I. The remaining 40% comprises the stroma-membrane fraction and contains PS I plus PS II_β. Moreover, we find that the properties of PS I in the two fractions are different in that the PS I in the grana fraction, PS I_α, has a larger functional antenna size than the PS I of the stroma-membrane fraction, PS I_β.

Materials and Methods

Chemicals

Dextran 500 was obtained from Pharmacia (Uppsala Sweden). Poly(ethylene glycol) 4000 (Carbovac PEG 3350) was supplied by Union Carbide (New York, NY).

Chloroplast isolation

Spinach plants (*Spinacia oleracea* L.) were grown at 20°C with a light period of 12 h. Chloroplasts were isolated by homogenizing samples of 30 g leaves for 5 s at maximum speed in a Turmix blender containing 100 ml of preparation medium (50 mM sodium phosphate buffer (pH 7.4)/5 mM MgCl₂/300 mM sucrose). The slurry was filtered through four layers of nylon mesh (25 μm) and centrifuged for 2 min at 1000 × g. The pellet was resuspended in preparation medium and centrifuged at 2000 × g for 5 min. The chloroplasts were resuspended and osmotically broken in 5 mM MgCl₂ followed by centrifugation at 2000 × g for 5 min. The thylakoid membranes obtained were washed twice in a buffer containing 10 mM Tricine (pH 7.4)/5 mM MgCl₂/300 mM sucrose. The membranes were then washed in a medium comprising 10 mM sodium phosphate buffer (pH 7.4)/5 mM NaCl/1 mM MgCl₂/100 mM sucrose, and finally resuspended in the same medium to give a concentration of about 4 mg Chl/ml.

Sonication

An aliquot of 1 ml of the thylakoid suspension was added to 10.66 g of a polymer mixture to yield 5.7% (w/w) Dextran 500/5.7% (w/w)

poly(ethylene glycol) 4000/10 mM sodium phosphate buffer (pH 7.4)/3 mM NaCl/1 mM MgCl_2 /20 mM sucrose. The polymer mixture was made in advance by mixing 3.32 g 20% (w/w) Dextran 500, 1.66 g 40% (w/w) poly(ethylene glycol) 4000, 0.53 g 0.2 M sodium phosphate buffer (pH 7.4), 0.30 g 0.1 M NaCl, 1.07 g 0.01 M MgCl_2 , 1.33 g 0.1 M sucrose and water to 10.66 g. The phase system containing thylakoids was sonicated in a Vibra-cell ultrasonic processor, Model VC 500 equipped with a $\frac{1}{2}$ -inch horn for 6×30 s with resting intervals of 1 min under continuous cooling. The ultrasonic exposure had an intensity output setting of 7, with 20% duty pulses. The sonication procedure started about 45 min after the thylakoids had been exposed to 1 mM MgCl_2 for the first time. To the sonicate containing thylakoid vesicles was finally added 1.43 g of pure lower phase to obtain equal volumes of the phases which then constituted the sample system.

Phase partitioning

The thylakoid vesicles were either separated by countercurrent distribution [18,27] or by a batch procedure in three steps. In both types of experiment a two-phase system of the following composition was used: 5.7% (w/w) Dextran 500/5.7% (w/w) poly(ethylene glycol) 4000/10 mM sodium phosphate buffer (pH 7.4)/5 mM NaCl/20 mM sucrose. The temperature was maintained at 4°C.

Countercurrent distribution. An apparatus where the phase separation is speeded up by centrifugation was used [28]. It contains 60 cavities, numbered 0–59. Equal amounts, 0.90 ml, of pure upper and lower phase were added to each of the cavities 5–59. Each of the cavities 0–4 was loaded with the sample system (1.80 ml). Each cycle comprised 30 s mixing and 90 s centrifugation, including one transfer. After 53 transfers the fractions were diluted with 1.80 ml 10 mM sodium phosphate buffer (pH 7.4)/5 mM NaCl/100 mM sucrose in order to break the phase systems. The diluted fractions were collected and the relative chlorophyll content for each fraction was tested by measuring the absorbance at 680 nm. Fractions 0–26 and 46–59 were pooled, further diluted and spun down ($100\,000 \times g$ for 90 min). The pellets were finally resuspended in a suitable buffer.

Batch procedure. Pure upper and lower phase (5 ml of each phase) was added to the sample system. The phase system was mixed thoroughly and separated under low-speed centrifugation ($1000 \times g$ for 3 min). The upper phase (T1) and lower phase (B1) were collected and repartitioned twice with 10 ml of pure lower and upper phase, respectively, yielding the T3 and B3 fractions. The thylakoid vesicles were removed from the polymers by 3-fold dilution in a buffer containing 10 mM sodium phosphate buffer (pH 7.4)/5 mM NaCl/100 mM sucrose and pelleted at $100\,000 \times g$ for 90 min. The pellets were finally resuspended in a suitable buffer.

Analysis

Determination of the chlorophyll was carried out according to Arnon [29].

Protein was determined with a modified Bearden [30] procedure, using Triton X-100 to solubilize membrane proteins [31].

SDS-polyacrylamide gel electrophoresis was performed in the buffer system of Laemmli [32] in the presence of 4 M urea in the gel, as described elsewhere [33].

Absorbance difference measurements for the quantification of P700 were obtained with an Aminco DW-2 spectrophotometer operated in a split-beam mode. The P-700 concentration was measured from the amplitude of the light-minus-dark absorbance change at 700 nm [34]. A difference absorption coefficient of $64 \text{ mM}^{-1} \cdot \text{cm}^{-1}$ was used [35]. The reaction mixture contained 0.02% (w/w) SDS, 2 mM methylviologen, 2 mM sodium ascorbate, 15 mM Tricine (pH 7.8), 10 mM NaCl, 400 mM sucrose and thylakoid membranes to yield about 20 μM chlorophyll.

Cytochrome *f* was determined by both a spectroscopic and an immunological method.

The concentration of photochemically active cytochrome *f* was determined with an Aminco DW-2 spectrophotometer, operated in a split-beam mode, from reduced-minus-oxidized absorbance change at 554 nm [36]. An absorption coefficient of $17.7 \text{ cm}^2 \cdot \text{mmol}^{-1}$ was used. The reaction mixture contained 1% (w/v) Triton X-100, 8 mM sodium phosphate buffer (pH 7.4), 4 mM NaCl, 80 mM sucrose and thylakoid membranes to yield a chlorophyll concentration of 50–150 μM . Fol-

lowing registration of the base line, hydroquinone (from a 100 mM stock) was added to the sample cuvette to yield a concentration of 2.4 mM. An equal volume of potassium ferricyanide (from a 100 mM stock) was added to the reference cuvette.

Antiserum against cytochrome *f* from spinach (Sigma) was raised in rabbits. The specificity of the serum was determined by Western blotting [37]. Thylakoid polypeptides were separated by SDS-polyacrylamide gel electrophoresis and transferred to a nitrocellulose membrane by electrophoresis. The blot was then cut into strips. One strip was stained with Amido black and the others were incubated with antiserum (2–10 μ l serum/10 ml medium) and peroxidase-conjugated goat anti-rabbit IgG. As a control, serum from a non-immunized rabbit was used. The bands containing peroxidase were developed by incubating the strips with H_2O_2 and *o*-dianisidine. Rocket immunoelectrophoresis [38] was run according to Anderson et al. [39] at pH 8.6. The concentration of the cytochrome *f* standard (Sigma) was determined spectrophotocally.

Electron transport measurements were made polarographically using a Clark-type O_2 electrode. PS I electron transport from reduced DCIP to methylviologen was measured in a medium comprising 40 mM sodium phosphate buffer (pH 7.4), 1 mM NaCl, 0.6 mM NaN_3 , 0.12 mM methylviologen, 0.3 mM DCIP, 32 mM ascorbate, 10 μ M DCMU, 2 mM NH_4Cl and thylakoid membranes to a chlorophyll concentration of 25 μ M. PS II electron transport from H_2O to PpBQ was measured in the presence of 30 mM sodium phosphate buffer (pH 6.5), 3 mM NaCl, 0.2 mM PpBQ, 60 mM sucrose and thylakoid membranes to a chlorophyll concentration of 25 μ M. Excitation light was passed through a 630 nm cut-off filter (RG 630). The light intensity was varied using a Regavolt variable transformer and Beckman's neutral filters and the photon flux densities were measured with a LI-COR (LI-170) quantum meter. Samples for electron microscopy were fixed overnight at 4°C with 1% osmium tetroxide, dehydrated with acetone and embedded in epoxy resin (Agar 100; Agar Scientific, U.K.). Thin sections were stained with 5% uranyl acetate at room temperature for 45 min and studied with a Philips EM 300 electron microscope working at 60 kV.

Kinetics of P-700 photooxidation was performed by the method described in Ref. 40. The potassium cyanide treatment of isolated membrane vesicles was performed according to Ref. 41 using 150 mM KCN for 2 h. The kinetics were measured with a DW-2 Aminco spectrophotometer working in dual-wavelength mode with 700 nm as measuring wavelength and 730 nm as reference. The optical path-length of the cuvette for the measuring beam was 10 mm and for the actinic beam it was 4 mm. The measuring beams were transmitted by a RG 695 Schott filter and a 695 nm interference filter HBW 70. The actinic beam (about 30 $\mu E \cdot m^{-2} \cdot s^{-1}$) was transmitted by a broad band filter, 380–600 nm, and a 566.9 nm interference filter HBW 80 to give a uniform light between 500 nm and 600 nm. Signal averaging was performed with a Nicolet instrument corporation (NIC) model 527. The reaction mixture contained 100 mM sucrose, 10 mM Tricine (pH 7.8), 1 mM $MgCl_2$, 50 μ M DCMU, 200 μ M methylviologen and 30 μ M chlorophyll.

Results

The diagram of the countercurrent distribution of sonicated thylakoids shows two well-separated peaks (Fig. 1). The one to the left, fraction numbers 0–26, and here designated α , contains about 60% and the one to the right, fraction numbers 46–59 and designated β , about 40% of the chloro-

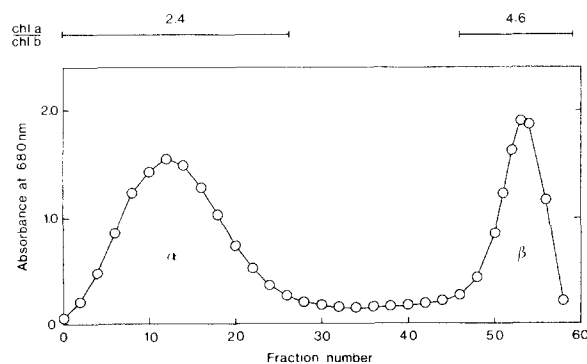


Fig. 1. Countercurrent distribution diagram of sonicated thylakoids. Note the chlorophyll *a/b* ratio of samples pooled from adjacent cavity positions (top of figure). Chemical compositions and photochemical activities of the fractions are shown in Tables I and II and Fig. 3.

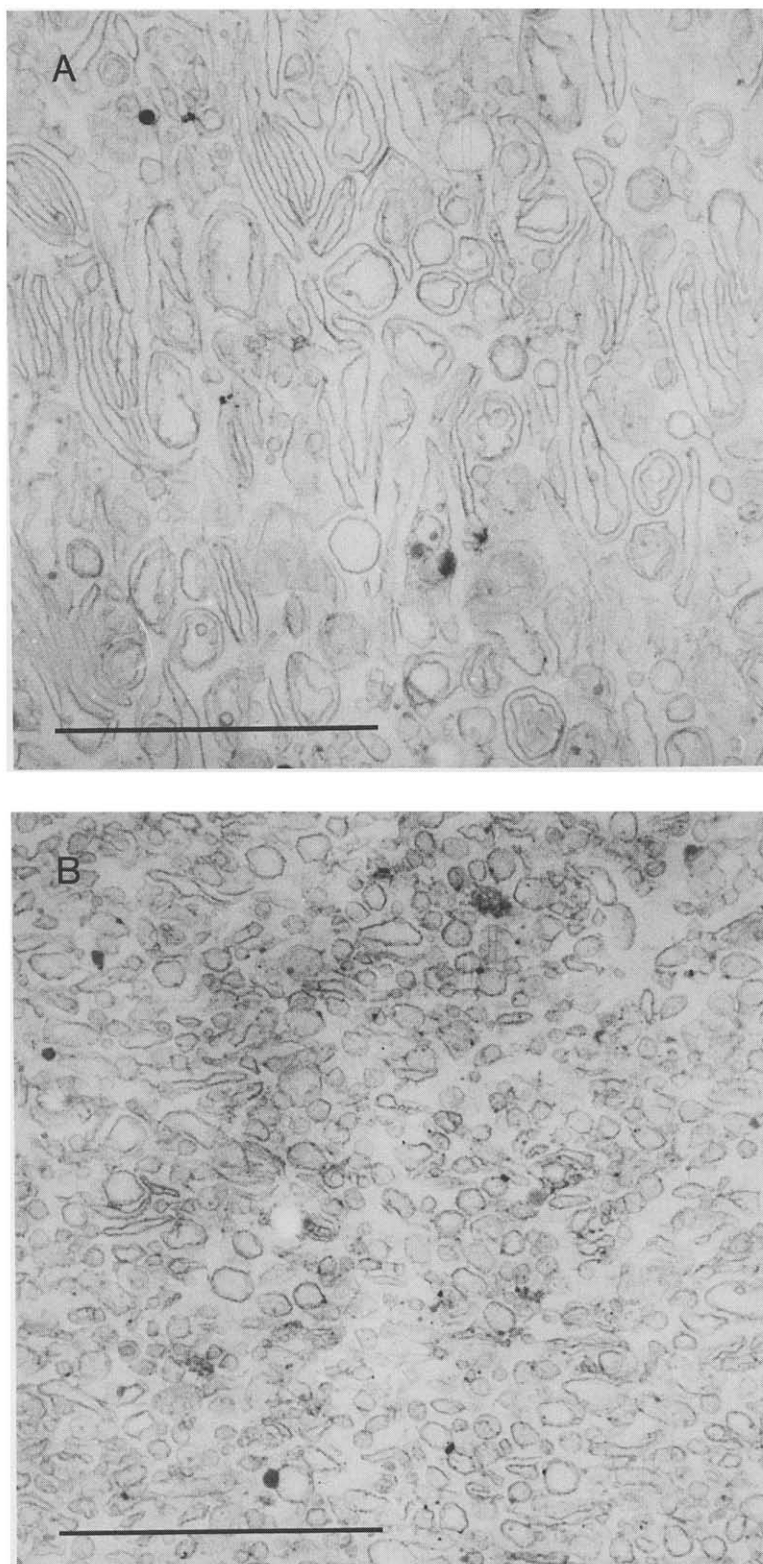


Fig. 2. Electron micrographs of pooled fractions from the CCD of Fig. 1: (A) fractions 0–26; (B) fractions 46–59. Bar represents 1 μm . The samples were fixed with osmium tetroxide, dehydrated with acetone and embedded in epoxy resin. Sections were stained with uranyl acetate.

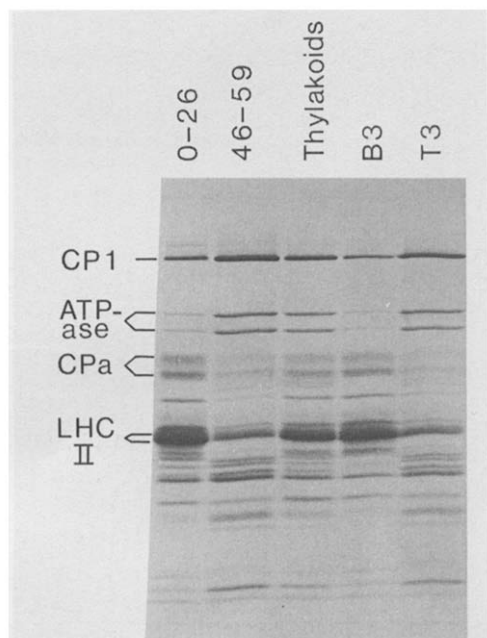


Fig. 3. Polypeptide profiles, as resolved by SDS-polyacrylamide gel electrophoresis. The first and the second track show the polypeptide patterns of pooled fractions from the CCD of Fig. 1. The two last tracks show the polypeptide patterns of fractions B3 and T3. CP1 (65 kDa) is a PS I polypeptide while CPa (43 and 47 kDa) and LHC II (25 and 27 kDa) are PS II polypeptides.

phyll. Very little material is found in the intermediate fractions, 27–45.

The average diameter of the α vesicles was considerably greater than that of the β vesicles (Fig. 2). The size of the α vesicles is of the same order of magnitude as grana partitions.

The α vesicles showed proton extrusion upon illumination, while the β vesicles showed proton uptake. This shows that the two fractions consist of vesicles with opposite sidedness, the α vesicles being 'inside-out' and the β 'right-side-out'.

The gel electrophoresis pattern demonstrates an enrichment of typical PS II polypeptides and depletion of PS I polypeptides in the α vesicles, while the opposite is demonstrated for the β vesicles (Fig. 3). There is, however, a significant amount of PS II polypeptides in the β vesicles and PS I polypeptides in the α vesicles. Cytochrome *f* is enriched slightly with PS II (Table I). This result, which was obtained both with the

spectrophotometric and the immunological method, agrees with previous reports showing that cytochrome *f* is slightly enriched together with PS II [16,18,19,42]. The immunological method gave a higher value of the cytochrome *f* content than the spectrophotometric one. The reason for this is not yet known to us.

The countercurrent distribution diagram shows that the α vesicles have a strong affinity for the lower phase, while the β vesicles have a strong affinity for the upper phase. The difference in partitioning between the two types of vesicle is so large that an efficient separation between them can be obtained by the batch procedure involving only three partition steps. This gives two main fractions, one from the lower phase (B3) and the other from the upper phase (T3), which correspond to the respective α and β peaks of the countercurrent distribution diagram. The biochemical and photochemical characterizations of these fractions show that the B3 fraction from the batch procedure is very similar to the α fraction of the countercurrent distribution procedure and, likewise, the T3 fraction is very similar to the β fraction (Tables I and II). The main difference between the two procedures is that with countercurrent distribution we can account for almost 100% of the material, while in the batch procedure we collect only 60% of the input material, since intermediate fractions are discarded. On the other hand, the batch procedure is somewhat faster.

The data of Table I and II show that the sonicated thylakoid membrane was separated into one fraction (B3 or 0–26) having typical grana membrane properties such as low chlorophyll *a/b* ratio, high PS II enrichment, slightly enriched in cytochrome *f*, and the other fraction (T3 or 46–59) with typical stroma membrane properties such as high Chl *a/b* ratio, high PS I enrichment and slightly depleted in cytochrome *f*. In this respect our results agree with previous results on Yeda-press-treated thylakoids [5–7,42].

The yields of about 60% grana-derived vesicles and 40% vesicles derived from stroma membranes agree approximately with the relative content of grana and stroma membranes *in vivo*. The fact that the vesicles of peak 0–26 were found to be considerably larger than the vesicles of peak 46–59 (Fig. 2) also indicates that the former originate

TABLE I

CHLOROPHYLL YIELD, CHLOROPHYLL *a/b* RATIO, PROTEIN, P-700 AND CYTOCHROME *f* CONTENT IN THE THYLAKOID MEMBRANE FRACTIONS

The membrane fractions were obtained after sonication and aqueous two-phase separation of spinach thylakoids. The phase separation was carried out by either countercurrent distribution (CCD) (Fig. 1) or a batch procedure in three steps. The chlorophyll yields of the two CCD fractions of Fig. 1 were estimated from their peak areas. The chlorophyll yields for the batch procedure and the chlorophyll *a/b* ratios were determined according to Arnon [29]. The protein content was determined by a modified procedure of Bearden [30]. P-700 concentration was measured from the amplitude of the light-minus-dark absorbance change at 700 nm [34]. The amount of cytochrome *f* was determined by both a spectroscopic (sp.) and an immunological (im.) method.

	Chlorophyll		Protein	P700	Cyt f	
	%	<i>a/b</i>	Chl	Chl	Chl	
		(mol/mol)	(g/g)	(mmol/mol)	(mmol/mol)	im. sp.
Thylakoids	100	3.1	5.7	2.6	2.4	1.3
CCD						
0–26	57	2.4	5.1	1.7	2.8	1.4
46–59	33	4.6	6.2	4.8	2.1	1.3
Batch						
B3	37	2.3	5.5	1.5	2.6	1.5
T3	21	5.0	6.8	4.7	1.9	1.2

from the grana and the latter from the stroma, since, on account of their compact and stacked structure, the grana should be more resistant to

TABLE II

PHOTOSYSTEM I AND PHOTOSYSTEM II ACTIVITIES FOR THE THYLAKOID MEMBRANE FRACTIONS

The PS I activity was measured from reduced DCIP to methylviologen. The PS II activity was measured from H₂O to PpBQ. Both activities (V_{\max}) are expressed as mol O₂/mol Chl per h. The k_m values were determined from the V/I vs. V plots.

	PS I activity		PS II activity	
	V_{\max}	k_m	V_{\max}	k_m
Thylakoids	504		135	
CCD				
0–26	156	44	171	412
46–59	747	78	45	921
Batch				
B3	124	27	257	604
T3	679	62	80	1127

disintegration by sonication than the stroma lamellae.

For both procedures there is a significant amount of PS I in the PS-II-enriched membranes (B3 and 0–26 fractions) and PS II in the PS-I-enriched membranes (T3 and 46–59 fractions); see Table I and Fig. 3.

From the distribution of chlorophyll between the two peaks (fractions 0–26 and 46–59 in Fig. 1) and the P-700 contents (Table I) one can calculate that about 35% of P-700 is in the grana-derived fraction and 65% in the stroma-membrane-derived fraction. For the PSI activity (V_{\max}) measurements, a similar calculation gives 26 and 74, respectively, for the per cent distribution of PS I between the two fractions. About 85% of the PS II is in the grana-derived fraction and 15% in the stroma-membrane-derived fraction. It was therefore of interest to study whether the properties of the two photosystems differed for the two types of vesicle. Such a comparison was performed by making light-saturation curves for the PS I and PS II activity and by studying the kinetics of photo-oxidation of P-700. Both these methods give information on the antenna size.

The light-saturation curves for oxygen evolution are shown in Fig. 4. The curves can be analysed by a V/I vs. V plot. For a homogeneous population of PS II centers this plot should give a straight line where the negative slope ($1/k_m$) is proportional to the value of the functional antenna size provided a constant turnover rate of the redox systems involved in the assay. The intercept

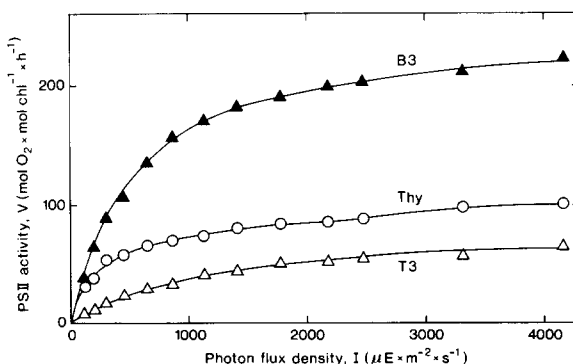


Fig. 4. PS II activity as a function of light intensity. The activity was measured from H₂O to PpBQ. ○, Thylakoids; ▲, B3 vesicles; △, T3 vesicles.

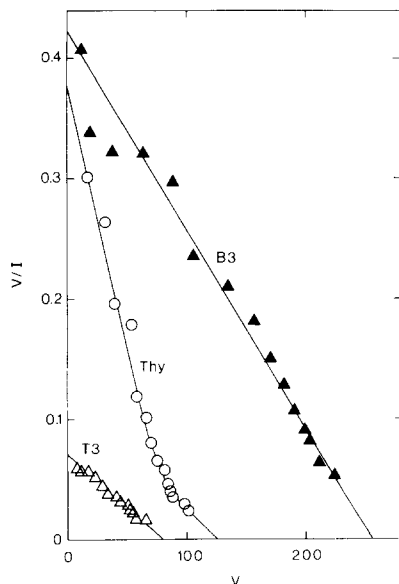


Fig. 5. V/I vs. V plot of the data from the PS II activity measurements of Fig. 4 (V is the PS II activity in $\text{mol O}_2/\text{mol Chl per h}$ and I is the light intensity). The intercept on the ordinate is V_{\max}/k_m and the intercept on the abscissa is V_{\max} . The slope is $-1/k_m$ where k_m is the light intensity that gives half-maximum activity; its inverse value is proportional to the functional antenna size. \circ , Thylakoids; \blacktriangle , B3 vesicles; \triangle , T3 vesicles. Note that the slope for the B3 vesicles is about twice as steep as that for the T3 vesicles.

on the abscissa, V_{\max} , is the maximal activity, K_m is the light intensity at half V_{\max} , and the intercept on the ordinate is V/I at zero light intensity. The V/I vs. V plots for the two different fractions give straight lines with different slopes, the B3 fraction having a steeper slope than T3 (Fig. 5). The k_m value for the B3 fraction is about half that of the T3 fraction, i.e., the functional antenna size of the PS II units of the B3 fraction is about twice as large as that of the PS II units of the T3 fraction. The plot for the thylakoids, which were used as starting material for the fractionation, consists partly of a straight line and partly of an upward concave curve, indicative of a heterogeneity in the antenna size of PS II. The thylakoids contain two classes of Photosystem II, PS II $_{\alpha}$ and PS II $_{\beta}$ [24,25] and our results of Fig. 5 can be interpreted such that the curve for the thylakoids is composed of at least two components, one representing PS II $_{\alpha}$ and the other PS II $_{\beta}$. The line

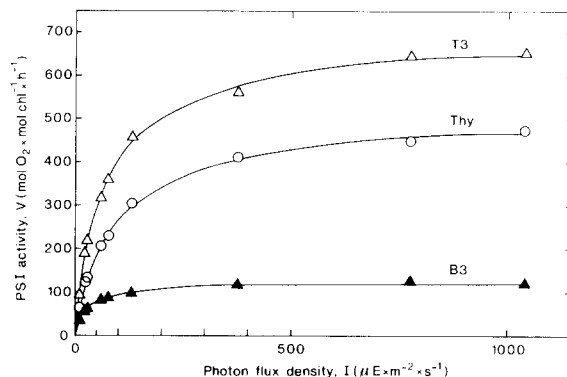


Fig. 6. PS I activity as a function of light intensity. The activity was measured from reduced DCIP to methylviologen. \circ , Thylakoids; \blacktriangle , B3 vesicles; \triangle , T3 vesicles.

for the B3 fraction represents PS II $_{\alpha}$ and that of the T3 fraction PS II $_{\beta}$.

The light-saturation curve for PSI activity (Fig. 6) shows that the activity of the B3 fraction is saturated at a lower light intensity than both the T3 fraction and the thylakoids. The V/I vs. V plot (Fig. 7) for the thylakoids gives an upward concave curve. It can be considered to be com-

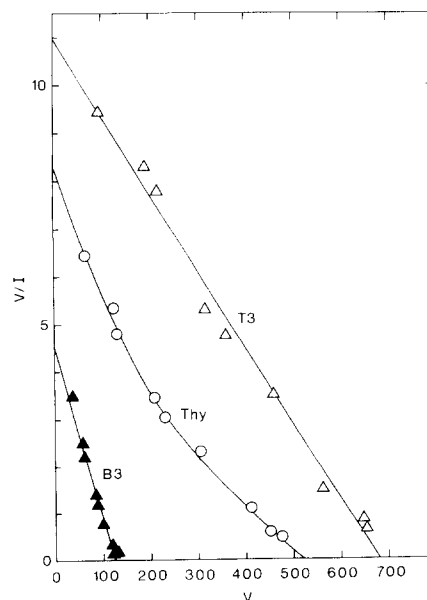


Fig. 7. V/I vs. V plot of the data from the PS I activity measurements of Fig. 6. For explanation of the plot see caption to Fig. 5. \circ , Thylakoids; \blacktriangle , B3 vesicles; \triangle , T3 vesicles. Note that the slope for the B3 vesicles is about twice as steep as that for the T3 vesicles.

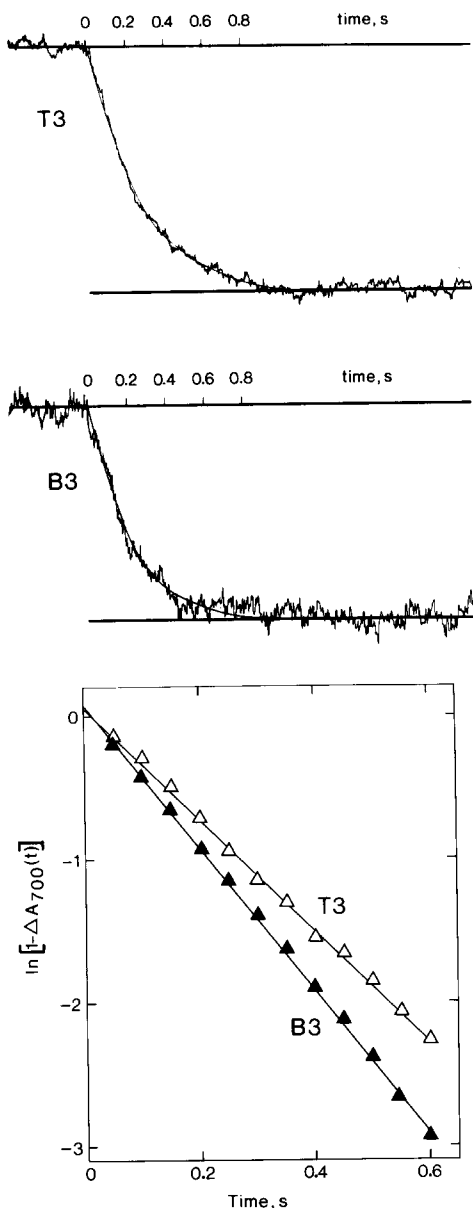


Fig. 8. (Upper) Kinetic traces: time-course of P-700 photooxidation. The actinic light came on at 0 s. The difference between the two horizontal lines in each trace represents the absorbance change at 700 nm, ΔA_{700} . The trace of T3 is the mean of eight individual measurements, while B3 is the mean of 21 individual measurements. Hand-drawn, best-fit curves were used for kinetic analysis. (Lower) First-order kinetic analysis of the traces above. B3 gave a higher rate constant (5.0 s^{-1}) than T3 (3.9 s^{-1}) as shown by the slopes of the lines in the semilogarithmic plot. \blacktriangle , B3; \triangle , T3.

posed of at least two parts, one with a steep slope and one with a flatter slope. The B3 and T3 fractions both give straight lines but with different slopes. The ratio between the k_m values is about 2, suggesting that the PS I units of the B3 fraction have a functional antenna size which is twice as large as that of the PS I units of T3; again with the assumption that the turnover rate of the redox components of the assay is the same for the two vesicle populations.

Similar results to those presented here for the B3 and T3 fractions were obtained with the α and β fractions from the countercurrent distribution experiment. The k_m values are presented in Table II. Thus, the PS I units of the two types of vesicle have different properties, and we propose names PS I $_{\alpha}$ and PS I $_{\beta}$, respectively. We also compared the kinetics of the P-700 photooxidation under weak illumination for the two vesicle populations. The rate constant for P-700 photooxidation is proportional to the antenna size of PS I and should be independent of the rate of electron transfer to P700 if plastocyanin is inhibited by KCN [40]. Fig. 8 shows typical kinetic traces of the time-course of P-700 photooxidation. The semilogarithmic plots for B3 and T3 both fit straight lines. The slopes of the lines are different and B3 displays about a 30% faster photooxidation than T3, indicating a similar difference in antenna size between PS I $_{\alpha}$ and PS I $_{\beta}$ under the light conditions used during the measurements.

Discussion

The main result of this work is that it demonstrates heterogeneity among PS I units in addition to the known heterogeneity among PS II units of chloroplasts. The PS I heterogeneity is demonstrated by two independent methods: Measurements of the PS I activity under different light intensities (light saturation curves) and studies of the kinetics of P-700 photooxidation.

Our two sonication-phase partitioning methods have both fractionated the thylakoid membrane into two well-separated vesicle populations, differing in morphology, biochemical composition and functional properties of PS I and PS II, which are both present in both populations. The one population, originating from the grana, contains

PS I $_{\alpha}$ and PS II $_{\alpha}$, which both have a functional antenna size larger than that of the corresponding PS I $_{\beta}$ and PS II $_{\beta}$ present in the other population, originating from the stroma membrane.

The main advantages with the two procedures are that they are relatively rapid, mild and quantitative. By using the apparatus designed by Åkerlund [28] the countercurrent distribution time is reduced to about 2 h, while our earlier countercurrent distribution experiments [5,42] needed 6–12 h. The batch procedure is even faster. The photosynthetic activities are well preserved in both procedures, but the highest activities were obtained with the batch procedure, probably because this takes a shorter time and requires less handling of the material. It is essential to carry out the sonication with the thylakoids present in the phase system, since this protects the photochemical activities.

It is a combination of sonication and phase partition which makes our new procedures superior to our previously published methods (using Yeda press treatment, see Ref. 14 for a review) particularly with respect to efficiency of separation, yield and reproducibility. The yield of about 40%, on a chlorophyll basis, of our peak to the right in Fig. 1, which represents stroma membranes, is a considerable improvement over conventional centrifugation methods, which only give a yield of a few per cent. Our T3 or 46–59 fraction can therefore be considered as reliably representative of the stroma membrane of the thylakoid. While we prefer the batch procedure when we wish to measure the photochemical activities or separate large quantities of vesicles, the countercurrent distribution is preferred when we wish to obtain a quantitative separation of the two vesicle populations. With the countercurrent distribution procedure we can account for almost 100% of the input material.

The light-saturation curve of the PS II activity shows heterogeneity among PS II units of the thylakoid membrane and gives independent additional support to the observation of at least two classes of PS II units, PS II $_{\alpha}$ and PS II $_{\beta}$, differing in antenna size [24]. In theory the steepest part of the thylakoid curve in Fig. 5 should have about the same (but not exactly the same) slope as the B3 fraction if PS II consists of only two classes,

PS II $_{\alpha}$ and PS II $_{\beta}$. We have no explanation of the fact that the thylakoid curve is steeper; it could be due to a larger overall antenna size and a better connectivity of the PS II $_{\alpha}$ units in the more native membrane compared to the fragments, or a difference in the turnover rate of the reaction centers. What is important in this context is that the thylakoid curve is not a straight line, showing heterogeneity among the PS II units, while the data from the separated fragments B3 and T3 fit straight lines. Moreover, our results also confirm the localization of PS II $_{\alpha}$ in the grana and PS II $_{\beta}$ in the stroma membranes [25].

The PSI units are also heterogeneous with respect to their antenna size, as evidenced by the thylakoid curve in the V/I vs. V plot (Fig. 7). The steeper slope of the thylakoid curve agrees fairly well with the slope of B3 considering that the PS I $_{\beta}$ makes some contribution to the PS I $_{\alpha}$ slope while the flatter slope of the thylakoid curve is more flat than the T3 line. Again, the main point in this context is that the data for the thylakoids do not fit a straight line, indicating heterogeneity among the PS I units, while the data for the fragments B3 and T3 fit straight lines with different slopes.

In addition, the difference in antenna size of PS I $_{\alpha}$ and PS I $_{\beta}$ was confirmed by the observed difference in the rate constants for the photo-oxidation of P-700 of the two fractions (Fig. 8), showing that at least two populations of PS I are present in the thylakoid membrane. The PS I $_{\alpha}$, having the largest antenna size, is present in the grana-derived vesicles while PS I $_{\beta}$, with its smaller antenna, is present in the stroma-membrane vesicles.

While our results clearly demonstrate heterogeneity among PS I, it is difficult at the present stage of our work to quantify these differences in terms of antenna size. If we assume constant turnover rate of the redox components of the PS I assay, the antenna size of PS I $_{\alpha}$ would be about 100% larger than that of PS I $_{\beta}$ as judged from the slopes of the lines in Fig. 7. Since the ratio between the V_{\max} of B3 and T3 differs from the ratio of P-700 for the two fractions, one can argue that the turnover rate of the PS I units of the two fractions differ. If we take this into account, then the antenna size of PS I $_{\alpha}$ would be about 30%

larger than that of PS I $_{\beta}$. (An alternative interpretation is that part of the P-700 in the B3 fraction is not photochemically active; in which case the antenna size of the remaining units would be higher.) The difference in rate constants of the photooxidation of P-700 points to a difference of about 30%. The light quality used for PS I activity measurements (red light) is different from the actinic light (green) used in the P-700 photooxidation measurements, so the two methods should not necessarily give the same antenna size if the pigment composition for PS I $_{\alpha}$ and PS I $_{\beta}$ differ. Further studies on PS I complexes isolated from the two membrane compartments have to be done in order to determine the exact chlorophyll-polypeptide composition of PS I $_{\alpha}$ and PS I $_{\beta}$ and their antenna size. It is of interest in this context that Bassi and Simpson [46] and Williams et al. [47] have isolated two types of PSI complex, one with and the other without a light-harvesting chlorophyll-protein complex, LHC II. The difference between PS I $_{\alpha}$ and PS I $_{\beta}$ might be that PS I $_{\alpha}$, unlike PS I $_{\beta}$, is associated with an LHC II complex, which could explain both its larger antenna size and its localisation in the grana region.

Heterogeneity among PSI units of chloroplasts from higher plants has, to our knowledge, not been described before. An indication of two discrete populations of PS I, with different cross-sections, in whole cells of *Chlorella vulgaris* has recently been described [43] and the antenna size of PS I differs for cells of *Macrocystis pyrifera* under different growth conditions [44]. Several studies by Melis and co-workers show that the photooxidation of P-700 in chloroplasts follows first-order kinetics with no sign of heterogeneity [45]. It may be, however, that with chloroplasts the PS I $_{\alpha}$ is not detected by studying the photooxidation of P-700 because it constitutes only a minor part compared to the dominating PS I $_{\beta}$ species. Armond and Arntzen [26] studied the antenna sizes of PS II and PS I in stroma and grana lamellae obtained by differential centrifugation of French-press-treated pea chloroplasts [26]. While they found that the PS II of the stroma and grana fractions saturated at different light intensities, indicative of different antenna sizes, no such difference was found for PS I in the two fractions. However, their grana fraction was obtained with a

yield of more than 90% of the thylakoid and had a chlorophyll *a/b* ratio of 2.86, and therefore, must have contained a large proportion of stroma lamellae. With their relatively high PS I activity, the contaminating stroma lamellae dominated the PS I behaviour of the grana fraction.

The P-700 of the grana derived fraction comprises 35% of the total P-700. At low light intensities, when light is the limiting factor for electron transport, the PS I $_{\alpha}$, with its larger antenna, will have an electron transport capacity which is comparable to that of PS I $_{\beta}$. Since the PS I units in the grana and stroma-membrane fractions differ in their antenna size, the PS I of the grana fraction can not merely be a contamination from the stroma membranes. They must somehow be associated with the PS II of the grana fraction and have a function different from the PS I of the stroma-membrane fraction. Our results show that the functional antenna sizes of PS I and PS II of the grana are larger than the corresponding antenna sizes of the stroma membrane. This suggests that the photosystems of the grana are designed to allow effective electron transport both at low and high light intensities, while the stroma-membrane photosystems work mainly at high light intensities as a supplement to the grana systems.

That the PS I $_{\alpha}$ and PS II $_{\alpha}$ units of the grana have larger antenna sizes than the corresponding PS I $_{\beta}$ and PS II $_{\beta}$ of the stroma membranes is consistent with the presence of relatively more grana stacks in chloroplasts of cells which live under low light conditions, such as cells of shade plants and cells of the lower part of a leaf [48].

We have shown elsewhere [15,18–23] that the PS I of inside-out vesicles obtained after press treatment most probably is localized in domains separate from PS II. Our results therefore suggest that the PS I $_{\alpha}$ units of the grana reside in domains separate from PS II $_{\alpha}$, such as the margins and the end membranes of the grana and even in domains of the partition region.

Acknowledgements

We thank Mrs. Agneta Persson and Mrs. Ingun Sunden-Cullberg for skillful technical assistance. This work was supported by the Swedish Natural Sciences Research Council.

References

- 1 Michel, J.M. and Michel-Wolwertz, M.R. (1968) in *Carnegie Institute Year Book*, 1967, pp. 508–516.
- 2 Sane, P.V., Goodchild, D.J. and Park, P.B. (1970) *Biochim. Biophys. Acta* 216, 162–178.
- 3 Jacobi, G. and Lehmann, H. (1968) *Z. Pflanz. Physiol.* 59, 457–476.
- 4 Anderson, J.M. and Boardman, N.K. (1966) *Biochim. Biophys. Acta* 112, 403–421.
- 5 Åkerlund, H.-E., Andersson, B. and Albertsson, P.-Å. (1976) *Biochim. Biophys. Acta* 449, 525–535.
- 6 Andersson, B., Åkerlund, H.-E. and Albertsson, P.-Å. (1977) *FEBS Lett.* 77, 141–145.
- 7 Andersson, B. and Åkerlund, H.-E. (1978) *Biochim. Biophys. Acta* 503, 462–472.
- 8 Andersson, B., Simpson, D.J. and Høyer-Hansen, G. (1978) *Carlsberg Res. Commun.* 43, 77–89.
- 9 Andersson, B., Sundby, C. and Albertsson, P.-Å. (1980) *Biochim. Biophys. Acta* 599, 391–402.
- 10 Vallon, O., Wollman, F.A. and Olive, J. (1985) *FEBS Lett.* 183, 245–250.
- 11 Vallon, O., Wollman, F.A. and Olive, J. (1986) *Photobiophys. Photobiophys.* 12, 203–220.
- 12 Goodchild, D.J., Anderson, J.M. and Andersson, B. (1985) *Cell Biol. Int. Rep.* 9, 715–721.
- 13 Andersson, B. and Anderson, J.M. (1980) *Biochim. Biophys. Acta* 593, 427–440.
- 14 Andersson, B., Sundby, C., Åkerlund, H.-E. and Albertsson, P.-Å. (1985) *Physiol. Plant.* 65, 322–330.
- 15 Albertsson, P.-Å. and Svensson, P. (1988) *Mol. Cell. Biochem.* 81, 155–163.
- 16 Anderson, J.M. and Malkin, R. (1982) *FEBS Lett.* 148, 293–296.
- 17 Atta-Asafo Adjei, E. and Dilley, R.A. (1985) *Arch. Biochem. Biophys.* 243, 660–667.
- 18 Albertsson, P.-Å. (1985) *Physiol. Veg.* 23, 731–739.
- 19 Melis, A., Svensson, P. and Albertsson, P.-Å. (1986) *Biochim. Biophys. Acta* 850, 402–412.
- 20 Albertsson, P.-Å., Svensson, P. and Persson, A. (1987) *Acta Chem. Scand.* B41, 134–136.
- 21 Svensson, P. and Albertsson, P.-Å. (1987) in *Progress in Photosynthesis Research* (Biggins, J., ed.), Vol. II, pp. 281–284, Martinus Nijhoff, Dordrecht.
- 22 Albertsson, P.-Å. (1987) *Chem. Scripta* 27B, 189–194.
- 23 Albertsson, P.-Å. (1988) *Q. Rev. Biophys.* 21, 61–98.
- 24 Melis, A. and Homan, P.H. (1978) *Arch. Biochem. Biophys.* 190, 523–530.
- 25 Anderson, J.M. and Melis, A. (1983) *Proc. Natl. Acad. Sci. USA* 80, 745–749.
- 26 Armond, P.A. and Arntzen, C.J. (1977) *Plant Physiol.* 59, 398–404.
- 27 Albertsson, P.-Å. (1986) *Partition of Cell Particles and Macromolecules*, 3rd Edn., John Wiley, New York.
- 28 Åkerlund, H.-E. (1984) *J. Biochem. Biophys. Methods* 9, 133–141.
- 29 Arnon, D.I. (1949) *Plant Physiol.* 24, 1–15.
- 30 Bearden, J.C., Jr. (1978) *Biochim. Biophys. Acta* 533, 525–529.
- 31 Kjellbom, P. and Larsson, C. (1984) *Physiol. Plant.* 62, 501–509.
- 32 Laemmli, U.K. (1970) *Nature* 227, 680–685.
- 33 Ljungberg, U., Henrysson, T., Rochester, C.P., Åkerlund, H.-E. and Andersson, B. (1986) *Biochim. Biophys. Acta* 849, 112–120.
- 34 Melis, A. and Brown, J.S. (1980) *Proc. Natl. Acad. Sci. USA* 77, 4712–4716.
- 35 Hiyama, T. and Ke, B. (1972) *Biochim. Biophys. Acta* 267, 160–171.
- 36 Bendall, D.S., Davenport, H.E. and Hill, R. (1971) *Methods Enzymol.* 23, 327–344.
- 37 Bittner, M., Kupferer, P. and Morris, C.F. (1980) *Anal. Biochem.* 102, 459–471.
- 38 Laurell, C.-B. (1966) *Anal. Biochem.* 15, 45–52.
- 39 Andersson, B., Larsson, C., Jansson, C., Ljungberg, U. and Åkerlund, H.-E. (1984) *Biochim. Biophys. Acta* 766, 21–28.
- 40 Melis, A. (1982) *Arch. Biochem. Biophys.* 217, 536–545.
- 41 Quitrakil, R. and Jzawa, S. (1973) *Biochim. Biophys. Acta* 305, 105–118.
- 42 Åkerlund, H.-E. and Andersson, B. (1983) *Biochim.* 725, 34–40.
- 43 Greenbaum, N.L. and Mauzerall, D. (1987) in *Progress in Photosynthesis Research* (Biggins, J., ed.), Vol. II, pp. 65–68, Martinus Nijhoff, Dordrecht.
- 44 Smith, B. and Melis, A. (1987) *Plant Physiol.* 84, 1325–1330.
- 45 Melis, A. and Ow, R.A. (1982) *Biochim. Biophys. Acta* 682, 1–10.
- 46 Bassi, R. and Simpson, D. (1987) *Eur. J. Biochem.* 163, 221–230.
- 47 Williams, R.S., Allen, J.F., Brain, A.P.R. and Ellis, R.J. (1987) *FEBS Lett.* 225, 59–66.
- 48 Terashima, I. and Inoue, Y. (1984) *Plant Cell Physiol.* 25, 555–563.